Near Infrared-Fluorescent and Magnetic Resonance Imaging Molecular Probe with High T1 Relaxivity for In Vivo Multimodal Imaging

Kevin Guo,[a] Mikhail Y. Berezin[a], Jie Zheng[a], Walter Akers[a], Franck Lin[b], Bao Teng,[c] Olga Vasalatiy,[c] Amir Gandjbakhche,[d] Gary L. Griffiths,[c] and Samuel Achilefu[a,b,e,*]

Departments of [a]Radiology, [b]Biomedical Engineering, and [d]Biochemistry & Molecular Biophysics Washington University, St. Louis, MO 63110, U.S.A. Fax: 314-747-5191; Tel: 314-362-8599; E-mail: achilefus@mir.wustl.edu

[c] Imaging Probe Development Center, NHLBI and [d] Eunice Shriver NICHD, National Institutes of Health, , Bethesda, MD 20892, U.S.A.

Electronic Supplementary Information

CONTENTS

I. IN VITRO STUDIES

A. Methods and materials

DMSO (spectrophotometric grade), $GdCl_3$ >99% purity, 1,1′,3,3,3′,3′-Hexamethylindotricarbocyanine iodide (HITC), and bovine serum albumin (BSA) (grade agarose gel electrophoresis, 99%) were obtained from Sigma-Aldrich (St. Louis, MO) and used without purification. LS479 was prepared as described previously[1]. Water 18.2 MΩ water from water purification system (Millipore, Billerica, MA) was used in all studies. UV/Vis spectra of samples were recorded using a DU-640 spectrophotometer (Beckman-Coulter), fluorescence spectra were recorded using a Fluorolog III fluorometer (Horiba Jobin Yvon Inc., Edison NJ) with excitation at 675 nm, scan 690-950 nm. Proton T_1 measurements were determined with a benchtop Maran NMR Scanner (Oxford Instruments, 23 MHz).

B. Synthesis and Spectroscopic Properties of LS479-Gd^{3+}

Formation of LS479-Gd^{3+}. Complex LS-479-Gd^{3+} was prepared by mixing stoichiometric quantities of LS479 and $GdCl_3$ in water and vigorously vortexing the mixture for 2 min and then shaking for 20 min. Complex formation was confirmed by monitoring the absorption spectra of the mixture. Upon complex formation, the absorption spectrum of LS479 undergoes a bathochromic shift as is shown in Fig. S1, left; the change stops at 1:1 molar ratio (Fig. S1, right)

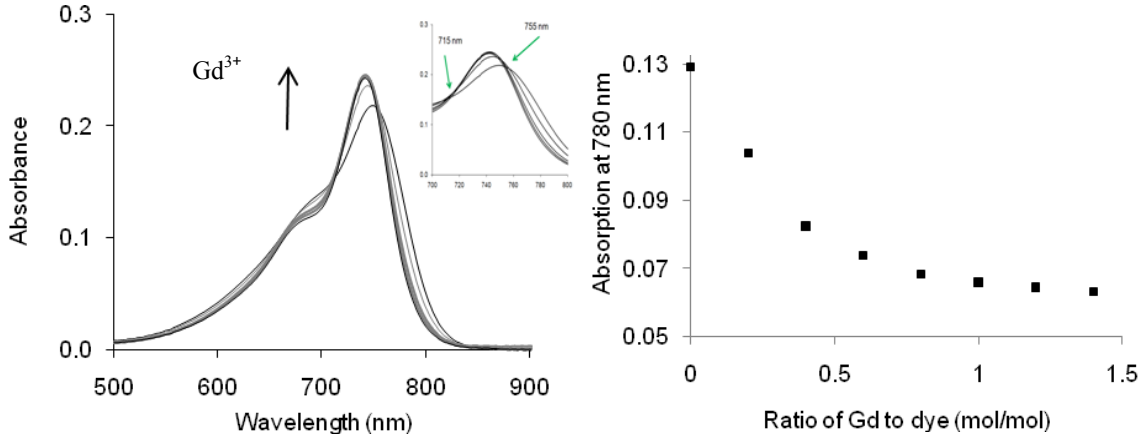

Figure S1: (Left panel) Titration absorbance spectra of LS479 with $GdCl_3$ in water. Black arrow indicates the direction of increasing Gd^{3+} concentration. The insert shows the presence of two isosbestic points (green arrows) at 715 nm and 755 nm. Bathochromic shift of ~10 nm with two isosbestic points at ~715 nm and 755 nm are shown. (Right panel) Absorbance, at 780 nm as a function of metal/dye ratio

Formation of LS479—albumin, LS479-Gd^{3+}-albumin complexes. LS479 and LS479-Gd^{3+} were added up to a concentration of 1 uM in a 1x1 cm quartz cuvette in a 2 mL solution of 40 mg/mL BSA in water to ensure complete complexation.

C. Evaluation of Binding Constants to Albumin

Albumin binding affinity of dyes was calculated based on tryptophan emission quenching. The theory of this is provided below.

Theory of Measuring Binding Constants to Albumin: Since the optical properties of tryptophan and the studied dyes do not overlap, the tryptophan fluorescence measurements are free from dyes'

interference. The linear relationship between albumin emission and concentration (R^2=0.99 for concentration between 0 to 2 mg/mL, not shown here) provided the necessary quantification basis to measure the binding constants. Thus, we assumed that the complexation between a NIR dye and BSA occurs according to Eq. S1.

$$BSA + nDye \rightleftarrows Dye_nBSA \quad \textbf{(S1)}$$

n - number of binding sites on albumin

The total concentration of BSA, BSA_{total}, is the sum of the concentrations of free albumin, BSA_{free}, in solution and the bound albumin:

$$[BSA_{total}] = [BSA_{free}] + [Dye_nBSA] \quad \textbf{(S2)}$$

Therefore, the binding constant K is expressed as follows:

$$K = \frac{[Dye_nBSA]}{[Dye]^n[BSA_{free}]} \quad \textbf{(S3)}$$

Combining eq. 2 and 3

$$\frac{[BSA_{total}] - [BSA_{free}]}{[BSA_{free}]} = K[Dye]^n \quad \textbf{(S4)}$$

Concentration of $[BSA_{total}]$ could be calculated from BSA fluorescence originating from the endogenous fluorophores tryptophan. Assuming each bound molecule causes complete quenching, then relative fluorescence $\frac{(F_0 - F)}{F}$ is proportional to the dye concentration.

$$\frac{(F_0 - F)}{F} = K[Dye]^n \quad \textbf{(S5)}$$

where F_o is the fluorescence of total albumin and F is the fluorescence of $[BSA_{free}]$

and finally, the number of binding sites can be calculated from a double logarithmic plot:

$$\log\frac{(F_0 - F)}{F} = \log K + n\log[Dye] \quad \textbf{(S6)}$$

where F_o - fluorescence of total BSA, F - fluorescence of free BSA, K – the binding constant, n a number of binding sites.

The number of binding sites from titration experiments can be evaluated using Eq. S6. The slope of the line generated by a double logarithmic plot. ICG, HITC and other cyanine dyes (not shown here) showed n values close to unity which indicates that only one site on the protein molecule could be occupied at one time and therefore the Eq. S5 could be simplified as:

$$\frac{(F_0 - F)}{F} = K[Dye] \quad \textbf{(S7)}$$

Experimental Measurement Binding Constants to Albumin: A stock solution of 0.08 mg/mL albumin was prepared by dissolving 2 mg into 25 mL of water and stored at 4 °C. For the binding measurements, 2 mL of albumin was added to a 1x1 cm quartz cuvette. Stock solutions of LS479, LS479-Gd^{3+}, and HITC were prepared and added to the albumin solution with small increments For LS479 and HITC, an equimolar concentration of NaCl was included to account for possible ionic effects After each addition of the probe, the resulting solution was mixed thoroughly and allowed to equilibrate for five minutes. Fluorescence was recorded with excitation at 279 nm (scan 294-450 nm).

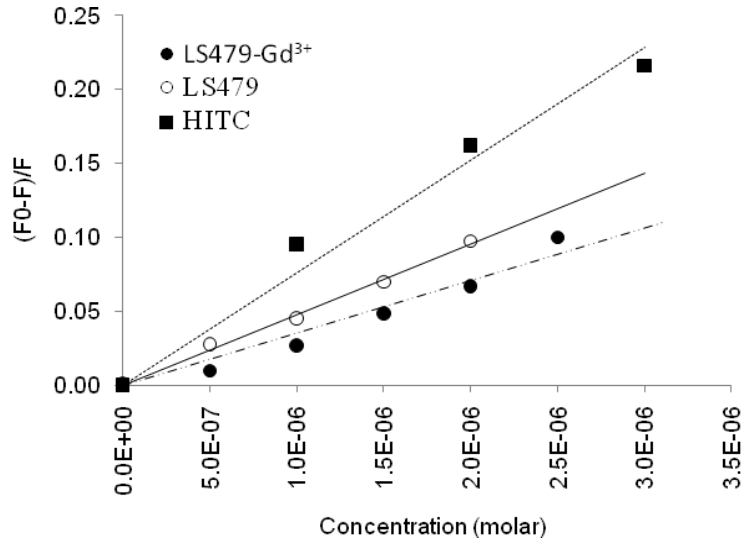

Figure S2 Measurement of binding of LS479, LS479-Gd^{3+} complex and HITC to albumin/water. LS479-Gd^{3+} (35,400 M^{-1}, R^2=0.96), LS479 (47,800 M^{-1}, R^2=0.99), HITC (76,300 M^{-1}, R^2=0.98).

D. In *vitro* T_1 relaxivity measurements

Proton T_1 measurements were determined with a benchtop Maran NMR Scanner (Oxford Instruments, 23 MHz, 37°C). A stock solution of 4% (40 mg/mL) albumin was prepared in 18.2 MΩ water. The measurements were conducted in a 1.5 mL solution of either water or albumin/water in a 10 mm diameter NMR tube. The solution was titrated with a contrast agent up to a concentration of 0.1mM. After each titration, the tube was thoroughly mixed and proton T_1 relaxivity was determined. Relaxivity values for contrast agents in albumin were adjusted by subtracting the relaxivity of albumin from the total relaxivity[2]. All relaxivity studies were done in triplicate and averaged.

E. Optical properties of LS479-Gd^{3+}-albumin complex

Solutions of LS479 and LS479-Gd^{3+} were characterized in a 4% solution of albumin in water. Large excess of albumin ([albumin]/[dye] ~ 500 mol/mol) and high binding constants (see below,) ensured the complete complexation of the dyes. Absorption and emission spectra in albumin were normalized and are shown in Fig. S3. LS479 and LS479-Gd^{3+} clearly differ in their absorbance and emission spectra, suggesting that LS479-Gd^{3+} does not dissociate when bound to albumin.

The quantum yields of LS479 and LS479-Gd^{3+} in 4% BSA were evaluated by comparison to ICG in DMSO (ψ=0.12) and, along with absorption and emission maxima, are given in Table S1. The differences in optical characteristics between LS479 and LS479-Gd^{3+} in albumin suggest that LS479-Gd^{3+} remains intact when bound to albumin and does not release free Gd^{3+}.

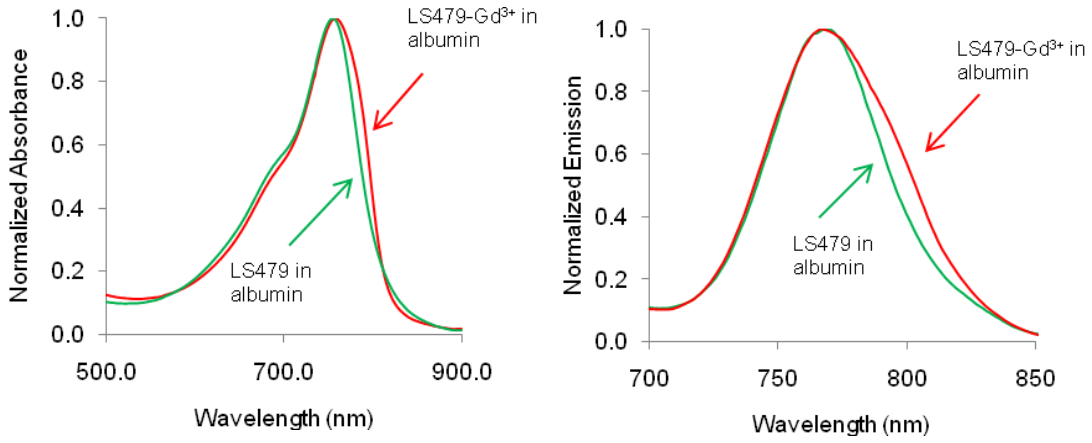

Figure S3: Absorption (left panel) and emission (right panel) spectra of LS479-Gd^{3+} stability when bound to albumin in water. (4% albumin solution). Ex. 675 nm, scan from 700 nm to 850 nm.

Table S1: Photophysical properties of LS479 and LS479-Gd^{3+} in 4% albumin in water.

Entry	Absorption max, nm	Emission max, nm	Quantum yield (ψ)
LS479	748	770	0.102
LS479-Gd^{3+}	758	767	0.124

Fluorescence Lifetime of LS479-$Gd3^{+}$ complex: Fluorescence lifetimes (FLT) were measured using time-correlated single-photon-counting (Horiba) with a 700 nm excitation source NanoLed® (impulse repetition rate 1 MHz) at 90º to the detector (Hamamatsu Photonics, Japan). For the FLT measurements, the dyes were dissolved in water and the absorbance of the measured solutions was maintained below 0.15 at a 700 nm excitation wavelength. The detector was set to 760 nm with a 26 nm bandpass and data collected until the peak signal reached 10,000 counts. The FL was recorded on a 50 ns scale. The instrument response function was obtained using a Rayleigh scatter of Ludox-40 (0.05% in water) in an acrylic transparent cuvette at 700 nm emission. Decay analysis software (DAS6 v6.1; Horiba) was used for lifetime calculations. The goodness of fit was judged by $\chi 2$ values, Durbin–Watson parameters, as well as visual observations of fitted line, residuals, and autocorrelation functions.

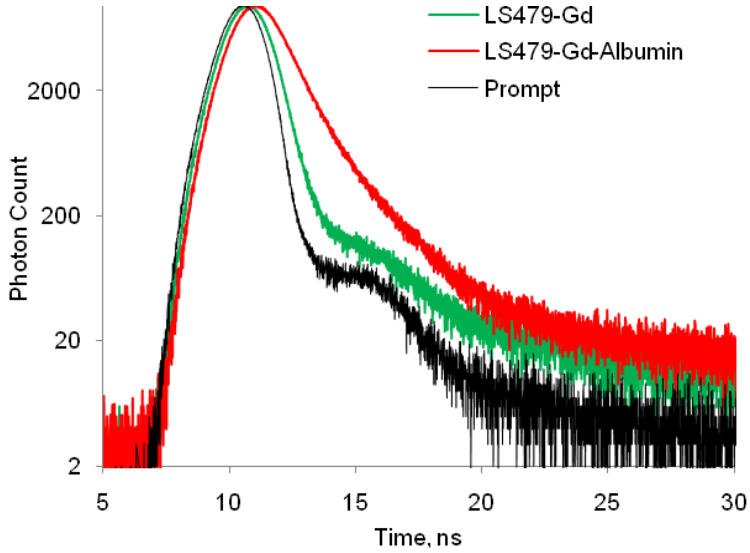

Figure S4: Lifetime decay curves of LS479-Gd^{3+} in water vs. LS479-Gd^{3+} in 4% albumin solution and the instrument response function (prompt).

Table S2 Fluorescence lifetime data of LS479-Gd^{3+} in water and 4% albumin in water.

	τ_1, ns	f_1, %	τ_2, ns	f_2, %	τ, ns	χ^2
LS479-Gd^{3+}	0.37	97.7	-	-	0.37	1.37
LS479-Gd^{3+}-albumin	0.69	54.8	1.31	43.2	0.95	

τ_1 – lifetime of the fast component, f_1 – fractional contribution of the fast component, τ_2 – lifetime of the slow component, f_2 – fractional contribution of the slow component, τ – average lifetime

II. IN VIVO STUDIES

A. General Methods

Animal studies were conducted in accordance with our animal protocol approved by Washington University Animal Studies Committee. LS479-Gd^{3+} was dissolved in 20% DMSO, 80% MΩ water to create a 2.5M solution. The mouse was anesthetized with intraperitoneal injection of ketamine and xylazine cocktail (87 mg/kg and 13 mg/kg, respectively). The contrast agent was administered by intravenous injection of 200 uL solution via lateral tail vein after pre-injection MR scan. After MRI, time-domain diffuse optical imaging was performed as described below with eXplore Optix, ART, Inc., Montreal, Canada multimodal imaging system. Fluorescence intensity and lifetime maps were superimposed on white light images acquired immediately before scanning.

The mouse was allowed to recover and optically imaged again 72 hours later. The animal did not show signs of pain or discomfort due to the contrast agent injection and appeared in good health at the time of sacrifice two months after injection.

B. MRI Imaging

MRI Data Acquisition: 3D FLASH MR images were acquired on 3 T Siemens Allegra head-only system using a single-channel volumetric coil (Nova Medical, Inc, Wilmington MA) with a diameter of 3 cm. The sequence parameters included: TR/TE = 10 msec/ 4 msec, flip angle = 40°, FOV = 50 x 50 mm, matrix = 256 x 256, 24 slices, slice thickness = 2mm, coronal scan, and bandwidth = 250 Hz/pixel. Scans were acquired prior to and immediately after contrast agent injection.

MRI Data Analysis: Three consecutive 3D scans were executed to study the dynamic changes in contrast-enhanced images at 2, 4, and 8 min. Signal to noise ratio (SNR) was measured in one slice of the 3D stack images showing two chambers of the heart. Regions-of-interest (ROIs) were placed on the myocardial septum, the liver, and the chest muscle to measure signal intensity. Another ROI was located in the air space outside body of the mouse without apparent flow artifacts. The standard deviation of this ROI signal was used as the noise. Figure S5 demonstrates ~100% and ~235% increases in SNR of myocardial septum and liver after 2 minutes, respectively. The T_1 signals for both the septum and liver then decay quickly, as illustrated by the T_1 weighted images at different time points (Figure 4, main text). Muscle signal shows minor changes over the time course observed.

Table S3 T_1 weighted signals from different organs in vivo and calculated Signal-to-Noise Ratio (SNR)

	T_1 Weighted Signals				SNR		
Time(min)	Heart	Liver	Muscle	Noise	Heart	Liver	Muscle
0	188.3	119.2	170.5	9.3	20.3	12.8	18.4
2	379.4	405.2	194.2	9.4	40.4	43.1	20.7
4	310.9	349.7	202.5	9.6	32.4	36.4	21.1
8	238.3	293.1	156.0	10.3	23.1	28.5	15.1

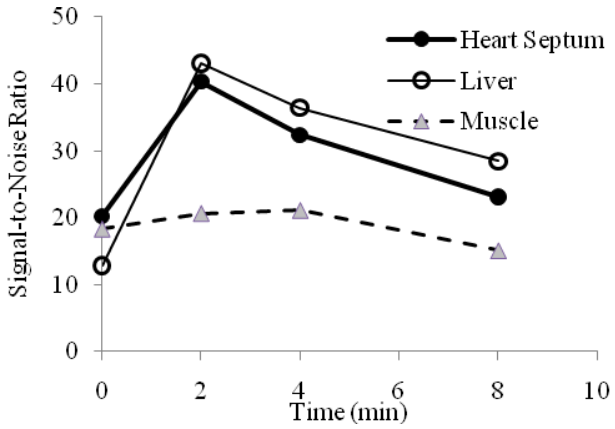

Figure S5: Raw data of T_1 weighted signal of selected ROI: heart septum, liver, and muscle.

C. Optical Imaging

Optical Data Acquisition: In vivo mouse images were acquired with a time-domain diffuse optical imaging system (eXplore Optix, ART, Inc., Montreal, Canada) as previously described.[3, 4] After

positioning the mouse on the heated imaging platform, a 2D scanning region was selected from the head to base of tail. Diffuse optical image data was acquired with point excitation at 780 nm and filtered 830 nm emission detection 3 mm from the excitation point. ROI were raster-scanned in 1.5 mm increments with 0.3 s integration time per pixel. Laser power was set to 0.4 μW for excitation scans and adjusted for optimal signal strength for each time point. Fluorescence scans were performed at 40 minutes and 72 hours after contrast agent administration.

Optical Data Analysis: Data analysis was performed using OptiView software (ART, Inc.) and displayed as fluorescence intensity (Fig. 5) or FLT (Fig. 6) maps with each pixel representing the integration of single exponential curve fitting of the acquired temporal point-spread function (TPSF), respectively, at each detection point. Pixels with less than 1 x 10^5 photon counts per second were not included in FLT measurement due to insufficient signal.

Table S4: ROI analysis of fluorescence image data showing the change in fluorescence lifetime at 40 minutes and 72 hours after injection. The fluorescence lifetime remained relatively unchanged in the neck, decreased slightly in the abdomen and back and decreased significantly in the kidney regions.

ROI	**Fluorescence lifetime (ns)**	
	40 minutes	72 hours
back	0.97	0.86
neck	0.97	0.91
kidney	0.98	0.67

References

1. M. Y. Berezin, K. Guo, B. Teng, W. B. Edwards, C. J. Anderson, O. Vasalatiy, A. Gandjbakhche, G. L. Griffiths and S. Achilefu, *J Am Chem Soc*, 2009, **131**, 9198-9200.
2. P. Caravan, J. C. Amedio, S. U. Dunham, M. T. Greenfield, N. J. Cloutier, S. A. McDermid, M. Spiller, S. G. Zech, R. J. Looby, A. M. Raitsimring, T. J. McMurry and R. B. Lauffer, *Chem Eur J*, 2005, **11**, 5866-5874.
3. W. Akers, F. Lesage, D. Holten and S. Achilefu, *Mol. Imaging*, 2007, **6**, 237-246.
4. S. Bloch, F. Lesage, L. McIntosh, A. Gandjbakhche, K. Liang and S. Achilefu, *J. Biomed. Opt.*, 2005, **10**, 54003.